

Top quark precision physics at the International Linear Collider*

D. Asner¹, A. Hoang², Y. Kiyo³, R. Pöschl^{†4}, Y. Sumino⁵ and M. Vos⁶

¹Pacific Northwest National Laboratory 902 Battelle Boulevard Richland, WA, USA

²Inst. für Theor. Physik, Universität Wien, Boltzmanngasse 5, A-1090 Vienna, AUSTRIA

³Department of Physics, Juntendo University, Inzai, Chiba 270-1695, JAPAN

⁴LAL, CNRS/IN2P3, Université Paris Sud, F-91898 Orsay CEDEX, FRANCE

⁵Graduate School of Science, Tohoku University, 6-3, Aramaki Aza-Aoba, Aoba-ku, Sendai 980-8578, JAPAN

⁶IFIC, Universitat de Valencia CSIC, c/ Catedrático José Beltrán, 2 46980 Paterna, SPAIN

Abstract

Top quark production in the process $e^+e^- \rightarrow t\bar{t}$ at a future linear electron positron collider with polarised beams is a powerful tool to determine the scale of new physics. Studies at the $t\bar{t}$ threshold will allow for precise determination of the top quark mass in a well defined theoretical framework. At higher energies vector, axial vector and tensorial CP conserving couplings can be separately determined for the photon and the Z^0 component in the electroweak production process. The sensitivity to new physics would be dramatically improved w.r.t. to what expected from LHC for electroweak couplings.

1 Introduction

The top quark, or t quark, is by far the heaviest particle of the Standard Model. Its large mass implies that this is the Standard Model particle most strongly coupled to the mechanism of electro-weak symmetry breaking. For this and other reasons, the

*This is a shortened version of the physics book for the ILC published in [1]. Where applicable updates of the results have been integrated.

[†]Corresponding author: poeschl@lal.in2p3.fr

Observable	Experiment	Value
Cross section $\sigma_{t\bar{t}}$	CDF [4]	7.82 ± 0.38 (stat.) ± 0.37 (syst.) ± 0.15 (th.) pb
	D0 [5]	$7.78 \pm^{+0.77}_{-0.64}$ (stat + syst. + lumi) pb
	ATLAS 7 TeV [6]	177 ± 3 (stat.) $^{+8}_{-7}$ (syst.) ± 7 (lumi.) pb
	ATLAS 8 TeV [7]	241 ± 2 (stat.) ± 31 (syst.) ± 9 (lumi.) pb
	CMS 7 TeV [8]	161.9 ± 2.5 (stat.) $^{+5.1}_{-5.0}$ (syst.) ± 3.6 (lumi.) pb
	CMS 8 TeV [9]	227 ± 3 (stat.) ± 11 (syst.) ± 10 (lumi.) pb
Top quark mass m_t	TEVATRON [10]	173.2 ± 0.51 (stat.) ± 0.71 (syst.) GeV
	LHC [11]	173.3 ± 0.5 (stat.) ± 1.3 (syst.) GeV
Top quark width Γ_t	CDF [12]	$2.21^{+1.84}_{-1.11}$ GeV
	D0 [13]	$1.99^{+0.69}_{-0.55}$ GeV
$BR(t \rightarrow Wb)/BR(t \rightarrow Wq)$	CDF [14]	0.94 ± 0.09
	D0 [15]	0.9 ± 0.04
	CMS [16]	$1.023^{+0.036}_{-0.034}$
Forward backward asymmetry A_{FB}^t	CDF [17]	0.162 ± 0.047 (stat. + syst.)
	D0 [18]	0.196 ± 0.060 (stat.) $^{+0.018}_{-0.026}$ (syst.)
Charge asymmetry A_C	ATLAS [19]	-0.018 ± 0.028 (stat.) ± 0.023 (syst.)
	CMS [20]	-0.013 ± 0.028 (stat.) $^{+0.029}_{-0.031}$ (syst.)
W boson helicity f_0	CDF [21]	0.726 ± 0.066 (stat.) ± 0.067 (syst.)
	ATLAS [22]	0.67 ± 0.03 (stat.) ± 0.06 (syst.)
	CMS [23]	0.698 ± 0.057 (stat.) ± 0.064 (syst.)

Table 1: Collection of recent results on $t\bar{t}$ production obtained at hadron colliders. The table reflects the status of the Winter conferences 2013.

t quark is expected to be a window to any new physics at the TeV energy scale. In this section, we will review the ways that new physics might appear in the precision study of the t quark and the capabilities of the ILC to discover these effects.

The t quark was discovered at the Tevatron proton-antiproton collider by the D0 and CDF experiments [2,3]. Up to now, the t quark has only been studied at hadron colliders, at the Tevatron and, only in past two years, at the LHC. The Tevatron experiments accumulated a data sample of about 12 fb^{-1} in Run I and Run II, at center of mass energies of 1.8 TeV and 1.96 TeV, respectively. About half of this data is fully analyzed. At the LHC, a data sample of about 5 fb^{-1} has been recorded at a center-of-mass energy of 7 TeV up to the end of 2011. In 2012, the machine has operated at a center of mass energy of 8 TeV. A non exhaustive collection of results obtained at hadron colliders is given in Table 1.

The ILC would be the first machine at which the t quark is studied using a precisely defined leptonic initial state. This brings the t quark into an environment in which individual events can be analyzed in more detail, as we have explained in the Introduction. It also changes the production mechanism for t quark pairs from the strong to the electro-weak interactions, which are a step closer to the phenomena of electro-weak symmetry breaking that we aim to explore. Finally, this change brings into play new experimental observables—weak interaction polarization and parity asymmetries—that are very sensitive to the coupling of the t quark to possible new

interactions. It is very possible that, while the t quark might respect Standard Model expectations at the LHC, it will break those expectations when studied at the ILC.

2 $e^+e^- \rightarrow t\bar{t}$ at threshold

One of the unique capabilities of an e^+e^- linear collider is the ability to carry out cross section measurements at particle production thresholds. The accurately known and readily variable beam energy of the ILC makes it possible to measure the shape of the cross section at any pair-production threshold within its range. Because of the leptonic initial state, it is also possible to tune the initial spin state, giving additional options for precision threshold measurements. The $t\bar{t}$ pair production threshold, located at a center of mass energy $\sqrt{s} \approx 2m_t$, allows for precise measurements of the t quark mass m_t as well as the t quark total width Γ_t and the QCD coupling α_s . Because the top is a spin- $\frac{1}{2}$ fermion, the $t\bar{t}$ pair is produced in an angular S -wave state. This leads to a clearly visible rise of the cross section even when folded with the ILC luminosity spectrum. Moreover, because the top pair is produced in a color singlet state, the experimental measurements can be compared with very accurate and unambiguous analytic theoretical predictions of the cross section with negligible hadronization effects. The dependence of the t quark cross section shape on the t quark mass and interactions is computable to high precision with full control over the renormalization scheme dependence of the top mass parameter. In this section, we will review the expectations for the theory and ILC measurements of the t quark threshold cross section shape. The case of the t quark threshold is not only important in its own right but also serves as a prototype case for other particle thresholds that might be accessible at the ILC.

2.1 Status of QCD theory

The calculation of the total top pair production cross section makes use of the method of non-relativistic effective theories. The t quark mass parameter used in this calculation is defined at the scale of about 10 GeV corresponding to the typical physical separation of the t and \bar{t} . This mass parameter can be converted to the \overline{MS} mass in a controlled way. The summation of QCD Coulomb singularities treated by a non-relativistic fixed-order expansion is well known up to NNLO [24] and has recently been extended accounting also for NNNLO corrections [25]. Large QCD velocity logarithms have been determined using renormalization-group-improved non-relativistic perturbation theory up to NLL order, with a partial treatment of NNLL effects [26,27,28]. Recently the dominant ultrasoft NNLL corrections have been completed [29,30,31]. The accuracy in this calculation is illustrated in Fig. 1.

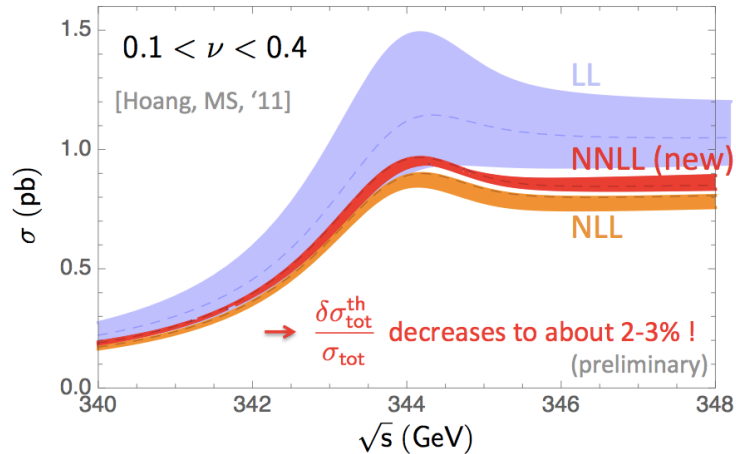


Figure 1: Accuracy on the prediction of the top pair production cross section at the $t\bar{t}$ threshold at the ILC as achieved by recent calculations of QCD corrections (NNLL). For further explanations see text. The figure has been taken from [32].

Since the t quark kinetic energy is of the order of the t quark width, electro-weak effects, which also include finite-lifetime and interference contributions, are crucial as well. This makes the cross section dependent on the experimental prescription concerning the reconstructed final state. Recently the NLO non-resonant calculation of $t\bar{t}$ production in [33,34] has been extended to NNLO accuracy [35,36].

Theoretical predictions for differential cross sections such as the top momentum distribution and forward-backward asymmetries are only known at the NNLO level and are thus much less developed.

2.1.1 Simulations and measurements

The most recent experimental study has been carried out by Seidel, Simon, and Tesar, for which the results are shown in Fig. 2 [37]. That study is based on a full detector simulation using the ILD detector. It takes the initial state radiation and beamstrahlung of the colliding beams into account. has been carried out by Martinez and Miquel in [38]. These authors assumed a total integrated luminosity of 100 fb^{-1} , distributed over 10 equidistant energy points in a 10 GeV range around the threshold, using the ILC and CLIC beam parameters. To treat the strong correlation of the input theory parameters, simultaneous fits were carried out for the t quark mass, the QCD coupling and the t quark width from measurements of the total cross section that was simulated based on the code TOPPIK with NNLO corrections [39]. The results are shown in Table 2 and demonstrate that the statistical precision of the t quark mass

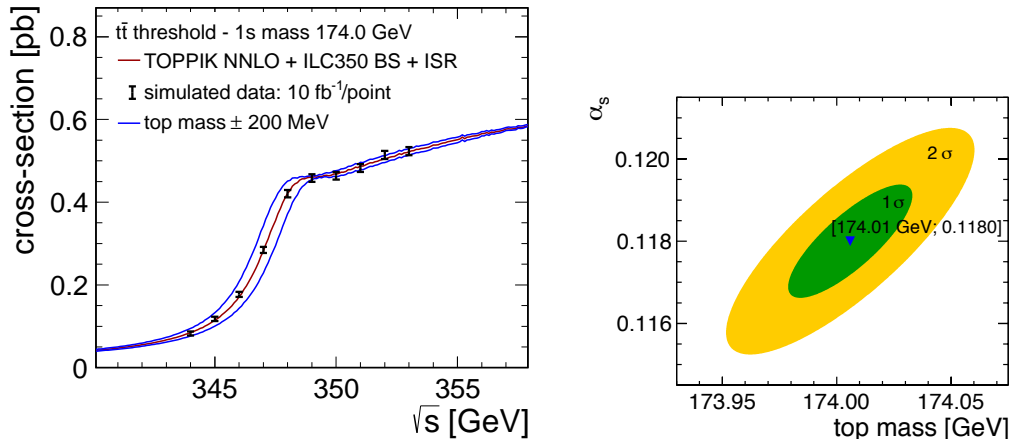


Figure 2: Illustration of a t quark threshold measurement at the ILC. In the simulation, the t quark mass has been chosen to be 174. GeV. The blue lines show the effect of varying this mass by 200 MeV. The study is based on full detector simulation and takes initial state radiation (ISR) and beamstrahlung (BS) and other relevant machine effects into account: (left) the simulated threshold scan. (right) error ellipse for the determination of m_t and α_s . The figure is taken from [37].

1S top mass and α_s combined 2D fit		
Error type	CLIC	ILC
m_t stat. error	27 MeV	34 MeV
m_t theory syst. (1%/3%)	5 MeV / 9 MeV	5 MeV / 8 MeV
α_s stat. error	0.0008	0.0009
α_s theory syst. (1%/3%)	0.0007 / 0.0022	0.0008 / 0.0022

Table 2: Results summary for the 2D simultaneous top mass and α_s determination with a threshold scan at CLIC and ILC for 10 points with a total integrated luminosity of 100 fb⁻¹ [37].

in this study is of the order of 30 MeV.

As shown in an older study by Martinez and Miquel in [38] even better precision may be achieved by taking other observables into account.

The threshold t quark mass determined in the study of Seidel et al. must still be converted to the standard t quark \overline{MS} mass. The conversion formula, to three-loop order, is given in [39]. The conversion adds an error of about 100 MeV from truncation of the QCD perturbation series and an error of 70 MeV for each uncertainty of 0.001 in the value of α_s . Both sources of uncertainty should be reduced by the time of the ILC running. In particular, the study of event shapes in $e^+e^- \rightarrow q\bar{q}$ at the high

energies available at ILC should resolve current questions concerning the precision determination of α_s . We recall that these estimates are the results of a precision theory of the relation between the threshold mass and the t quark \overline{MS} mass. A comparable theory does not yet exist for the conversion of the t quark mass measured in hadronic collisions to the \overline{MS} value.

The precise determination of the t quark mass is likely to have important implications for fundamental theory. A value of the top quark mass accurate at the level that a linear collider will provide is for example a key input to models of the vacuum stability of the universe.

3 Probing the top quark vertices at the ILC

At higher energy, the study of $t\bar{t}$ pair production concentrates on the precise measurements of the couplings of the t quark to the Z^0 boson and the photon. In contrast to the situation at hadron colliders, the leading-order pair production process $e^+e^- \rightarrow t\bar{t}$ goes directly through the $t\bar{t}Z^0$ and $t\bar{t}\gamma$ vertices. There is no concurrent QCD production of $t\bar{t}$ pairs, which increases greatly the potential for a clean measurement. A commonly used expression to describe the current at the $t\bar{t}X$ vertex is [40]

$$\Gamma_\mu^{t\bar{t}X}(k^2, q, \bar{q}) = ie \left\{ \gamma_\mu \left(\tilde{F}_{1V}^X(k^2) + \gamma_5 \tilde{F}_{1A}^X(k^2) \right) + \frac{(q - \bar{q})_\mu}{2m_t} \left(\tilde{F}_{2V}^X(k^2) + \gamma_5 \tilde{F}_{2A}^X(k^2) \right) \right\}. \quad (1)$$

where $X = \gamma, Z$ and the \tilde{F} are related to the usual form factors F_1, F_2 by

$$\tilde{F}_{1V}^X = - (F_{1V}^X + F_{2V}^X), \quad \tilde{F}_{2V}^X = F_{2V}^X, \quad \tilde{F}_{1A}^X = -F_{1A}^X, \quad \tilde{F}_{2A}^X = -iF_{2A}^X. \quad (2)$$

In the Standard Model the only form factors which are different from zero are $F_{1V}^\gamma(k^2)$, $F_{1V}^Z(k^2)$ and $F_{1A}^Z(k^2)$. The quantities $F_{2V}^{\gamma,Z}(k^2)$ are the electric and weak magnetic dipole moment (EDM and MDM) form factors. The presence of the γ/Z^0 interference in electro-weak production gives sensitivity to the actual sign of the coupling constants. This is a distinct difference to the associated vector boson production at the LHC, which is only sensitive to their absolute values.

In the following section, we will review the importance of measuring these couplings precisely. Then we will describe studies of the experimental capabilities of the ILC to perform these measurements. A great asset to test the chiral structure is the

availability of polarized beams at the ILC. The studies presented in the following exploit this potential. For a full overview on the physics potential with polarised beams the reader is referred to [41].

3.1 Top quark and new physics - A brief motivation

Neither the Standard Model of particle physics nor its super-symmetric extensions deliver an explanation for the striking mass hierarchy in the fermion sector. On the other hand, the mass hierarchy can be accommodated in models featuring extra dimensions, which are dual to models in which the t quark and the Higgs Boson are composited objects. An example model with extra dimensions is that by Randall and Sundrum [42]. New physics will modify the electro-weak $Z^0 t\bar{t}$ vertex and modify the couplings Q_L and Q_R to the left- and right-chiral parts of the t -quark wavefunction. New physics may also entail the existence of a new $Z^{0'}$ boson or Kaluza-Klein excitations of the Standard Model Z^0 boson. The modified vertex gives rise to different forward backward asymmetries A_{FB} than those predicted by the Standard Model. For this quantity a 3σ discrepancy of the effective electro-weak mixing angle $\sin^2\theta_{eff}$ obtained in $b\bar{b}$ production at LEP has yet to be resolved [43]. If this effect is real, it is likely to be larger for the heavy t quark. Please note that tensions with the Standard Model are also reported for the Tevatron results on A_{FB} in $t\bar{t}$ final states. The Standard Model prediction of the weak mixing angle is also challenged by the about 3σ discrepancy observed in the left right asymmetry A_{LR} at the linear collider SLC, which featured linearly polarized electron beams. This measurement is the most precise measurement of $\sin^2\theta_{eff}$ as of today.

3.2 ILC measurements

In the previous section, theories with extra dimensions and/or in which the t quark and the Higgs boson are composite were briefly introduced. Compositeness is an essential element of the physics of electro-weak symmetry breaking. A key test of this idea would come from the measurement of the $t\bar{t}Z$ couplings, where significant deviations from the predictions of the Standard Model would be expected. The ILC provides an ideal environment to measure these couplings. At the ILC $t\bar{t}$ pairs would be copiously produced, several 100,000 events for an integrated luminosity of 500 fb^{-1} . The production is by s -channel γ and Z^0 boson exchange, so the couplings to the Z^0 enter the cross section in order 1. It is possible to almost entirely eliminate the background from other Standard Model processes.

With the use of polarized beams, t and \bar{t} quarks oriented toward different angular regions in the detector are enriched in left-handed or right-handed t quark

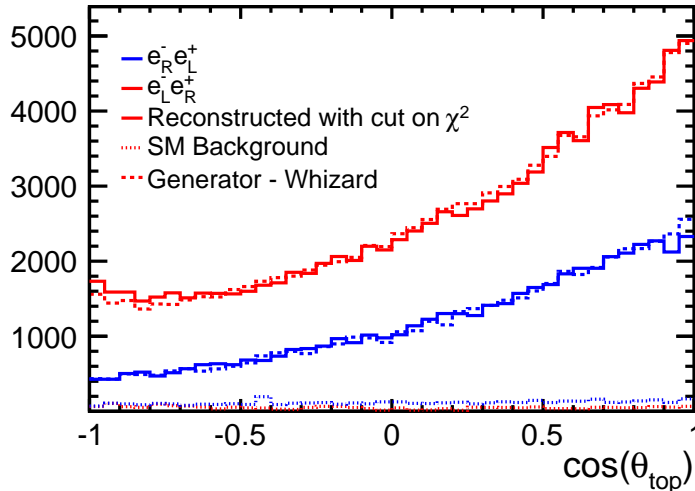


Figure 3: Reconstruction of the direction of the t quark for two different beam polarization [45]. The population in the two different hemispheres w.r.t. the polar angle θ_{top} allows for the measurement of the forward-backward asymmetry A_{FB} . The residual Standard Model background is very small.

polarization [44]. This means that the experiments can independently access the couplings of left- and right-handed polarized quarks to the Z^0 boson. In principle, the measurement of the cross section and forward-backward asymmetry for two different polarization settings measures both the photon and Z^0 boson couplings of the t quark for each handedness. New probes of the t quark decay vertices are also available, although we expect that these will already be highly constrained by the LHC measurements of the W polarization in t quark decay.

Recent studies based on full simulation of ILC detectors for a center of mass energy of $\sqrt{s} = 500$ GeV demonstrate that a precision on the determination of the couplings the left and the right chiral parts of the t quark wave function to the Z^0 boson of up to 1% can be achieved [46,47,48]. The most recent example for such a study of semi-leptonic $t\bar{t}$ decays with full detector simulation is shown in Figure 3 [45]. The figure demonstrates the clean reconstruction of the t quark direction, which allows for the precise determination of the forward-backward asymmetry, which is nearly free of Standard Model background. It has to be noted however, that the final state gives rise to ambiguities in the correct association of the b quarks to the W bosons, see [45] for an explanation. These ambiguities can be nearly eliminated by requiring a high quality of the event reconstruction. The control of the ambiguities however requires an excellent detector performance and event reconstruction. Another solution is the use of the vertex charge to separate the t and \bar{t} quark decays. It is shown in [47] and

confirmed in [49] that the high efficiency of vertex tagging in the ILC detectors will make this strategy available.

Even more incisive measurements than presented using optimized observables are investigated in [45]. These observables are the $t\bar{t}$ pair production cross-section for left- and right-handed polarized beams and the fraction of right-handed (t_R) and left handed t quarks (t_L). Following a suggestion by [50] for the Tevatron, the fraction of t_L and t_R in a given sample can be determined with the helicity asymmetry. In the t quark rest frame the distribution of the polar angle θ_{hel} of a decay lepton is

$$\frac{1}{\Gamma} \frac{d\Gamma}{d\cos\theta_{hel}} = \frac{1 + a_t \cos\theta_{hel}}{2} \quad (3)$$

where a_t varies between +1 and -1 depending on the fraction of right-handed (t_R) and left handed t quarks (t_L). The observable $\cos\theta_{hel}$ can easily be measured at the ILC. This observable is much less sensitive to ambiguities in the event reconstruction than the forward backward asymmetry. The slope of the resulting linear distribution provides a very robust measure of the net polarization of a t quark sample. The result of a full simulation study is shown in the top part of Fig. 4. It is demonstrated that over a range in $\cos\theta_{hel}$ the generated distribution is retained after event reconstruction. The reconstruction is nearly perfect for initial right handed electron beams. Remaining discrepancies in case of left handed electron beams can be explained by reconstruction inefficiencies for low energetic final state leptons.

The introduced observables, i.e. A_{FB} , cross sections and helicity asymmetry are used to disentangle the coupling of the t quark to the photon and to the Z^0 . In the bottom part of Fig. 4, the precision on the form factors expected from the LHC and that from the ILC are compared with each other.

Numerical values for the expected accuracies at linear e^+e^- colliders, ILC and earlier on TESLA [51], on seven t quark form factors (due to QED gauge invariance the coupling \tilde{F}_{1A}^γ is fixed to 0), taken from the studies [52,51,45], are given in Tabs. 3 and 4, along with comparisons to the expectations from the LHC experiments. Note in passing, that the replacement of TESLA results of Tab. 4 by an ILC study is in preparation.

From the comparison of the numbers it is justified to assume that the measurements at an electron positron collider lead to a spectacular improvement and thanks to the γ/Z^0 interference a e^+e^- collider can fix the sign the form factors. At the LHC the t quark couples either to the photon or to the Z^0 . In that case the cross section is proportional to e.g. $(F_{1V}^Z)^2 + (F_{1A}^Z)^2$. The precision expected at the LHC cannot exclude a sign flip of neither F_{1V}^Z nor of F_{1A}^Z . On the hand the LEP bounds can exclude a sign flip for F_{1A}^Z [53], which renders a much better precision for \tilde{F}_{1A}^Z compared with F_{1V}^Z . Clearly, the precisions that can be obtained at the LHC are to

Coupling	LHC [40]	e^+e^- [52]	e^+e^- [45]
	$\mathcal{L} = 300 \text{ fb}^{-1}$	$P_{e^-} = \pm 0.8$	$\mathcal{L} = 500 \text{ fb}^{-1}, P_{e^-,+} = \pm 0.8, \mp 0.3$
$\Delta \tilde{F}_{1V}^\gamma$	+0.043 -0.041	+0.047, $\mathcal{L} = 200 \text{ fb}^{-1}$ -0.047, $\mathcal{L} = 200 \text{ fb}^{-1}$	+0.002 -0.002
$\Delta \tilde{F}_{1V}^Z$	+0.24 -0.62	+0.012, $\mathcal{L} = 200 \text{ fb}^{-1}$ -0.012, $\mathcal{L} = 200 \text{ fb}^{-1}$	+0.002 -0.002
$\Delta \tilde{F}_{1A}^Z$	+0.052 -0.060	+0.013, $\mathcal{L} = 100 \text{ fb}^{-1}$ -0.013, $\mathcal{L} = 100 \text{ fb}^{-1}$	+0.006 -0.006
$\Delta \tilde{F}_{2V}^\gamma$	+0.038 -0.035	+0.038, $\mathcal{L} = 200 \text{ fb}^{-1}$ -0.038, $\mathcal{L} = 200 \text{ fb}^{-1}$	+0.001 -0.001
$\Delta \tilde{F}_{2V}^Z$	+0.27 -0.19	+0.009, $\mathcal{L} = 200 \text{ fb}^{-1}$ -0.009, $\mathcal{L} = 200 \text{ fb}^{-1}$	+0.002 -0.002

Table 3: Sensitivities achievable at 68.3% CL for the CP-conserving t quark form factors $\tilde{F}_{1V,A}^X$ and \tilde{F}_{2V}^X defined in (1), at LHC and at the ILC. The assumed luminosity samples and, for ILC, beam polarization, are indicated. In the LHC studies and in the study [52], only one form factor at a time is allowed to deviate from its SM value. In study [45] the form factors are allowed to vary independently.

be revisited in the light of the real LHC data. A first result on associated production of vector boson and $t\bar{t}$ pairs is published in [54].

Coupling	LHC [40]	e^+e^- [51]
	$\mathcal{L} = 300 \text{ fb}^{-1}$	$\mathcal{L} = 300 \text{ fb}^{-1}, P_{e^-,+} = -0.8$
$\Delta \text{Re} \tilde{F}_{2A}^\gamma$	+0.17 -0.17	+0.007 -0.007
$\Delta \text{Re} \tilde{F}_{2A}^Z$	+0.35 -0.35	+0.008 -0.008
$\Delta \text{Im} \tilde{F}_{2A}^\gamma$	+0.17 -0.17	+0.008 -0.008
$\Delta \text{Im} \tilde{F}_{2A}^Z$	+0.035 -0.035	+0.015 -0.015

Table 4: Sensitivities achievable at 68.3% CL for the t quark CP-violating magnetic and electric dipole form factors \tilde{F}_{2A}^X defined in (1), at the LHC and at linear e^+e^- colliders as published in the TESLA TDR. The assumed luminosity samples and, for TESLA, the beam polarization, are indicated. In the LHC studies and in the TESLA studies, only one form factor at a time is allowed to deviate from its SM value.

The expected high precision at a linear e^+e^- collider allow for a profound discussion of effects of new physics. The findings can be confronted with predictions in the framework of Randall-Sundrum models and/or compositeness models such as [55,56,57,58,59,60] or Little Higgs models as e.g. [61]. All these models entail deviations from the Standard Model values of the t quark couplings to the Z^0 boson that will be measurable at the ILC. The interpretation of the results presented in Tables 3 and 4 in terms of the cited and maybe other models is in preparation and left for a future publication. *Comments and contributions from theory groups are*

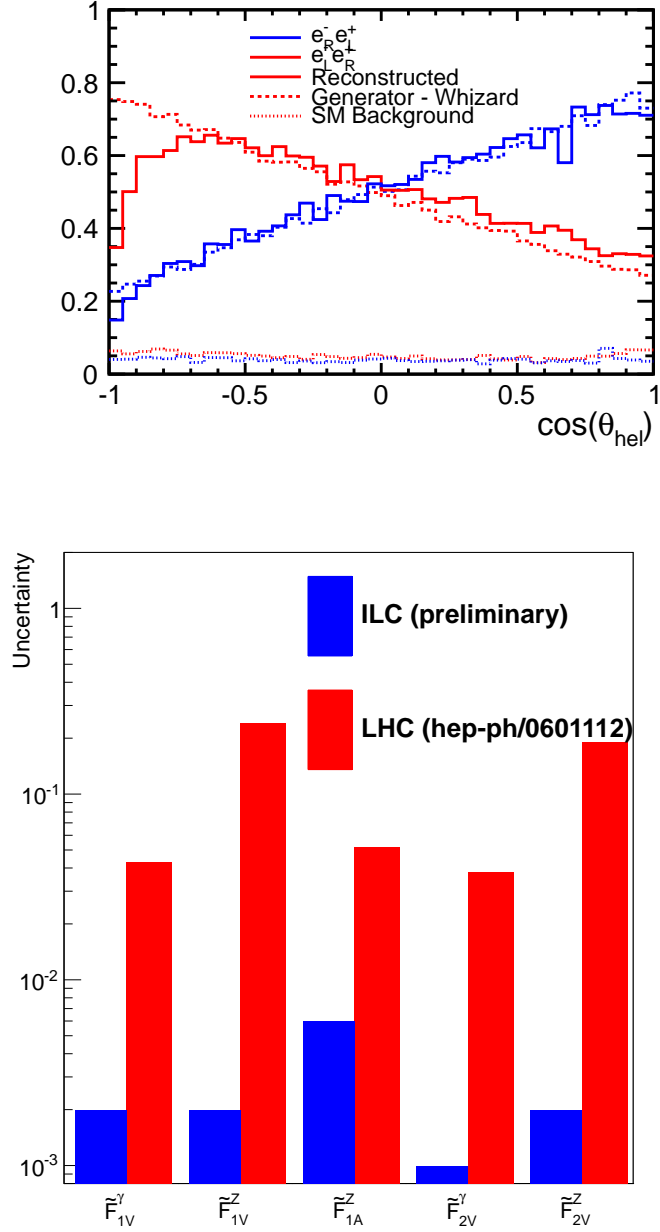


Figure 4: Top: Generated and reconstructed distribution of the helicity angle $\cos\theta_{hel}$; Bottom: Comparison of precisions on CP conserving form factors of the t quark to γ and Z , $\tilde{F}_{1V,A}^{\gamma,Z}$, expected at the LHC, taken from [40], and at the ILC. The LHC results assume an integrated luminosity of $\mathcal{L} = 300 \text{ fb}^{-1}$. The results for ILC [45] assume an integrated luminosity of $\mathcal{L} = 500 \text{ fb}^{-1}$ at $\sqrt{s} = 500 \text{ GeV}$ and a beam polarization $P_{e^-} = \pm 0.8$, $P_{e^+} = \mp 0.3$.

highly welcome.

3.2.1 Theory uncertainties on form factors - A brief outline

The extraction of form factors requires precise predictions of the inclusive $t\bar{t}$ production rate and several differential distributions. As of today the QCD corrections are known to N^3LO accuracy for the cross section and to $NNLO$ accuracy for A_{FB}^t . It is shown in [45] and references therein that the uncertainty on these corrections for the cross section are below 1% with an even smaller scale uncertainty. Uncertainties for A_{FB}^t yield about the same values.

Electro-weak corrections are known to NLO accuracy. The correction for the cross section is about 5% at $\sqrt{s} = 500$ GeV. The correction for A_{FB}^t is between 10% and 15% [62,63]. It is a major task for the future to estimate the size of the two-loop-correction and ultimately to calculate this contributions.

At this point it should also be noted that all of the studies on form factors are based on the WHIZARD event generator [64,65]. This generator provides the final state in terms of six fermion events. In particular the $t\bar{t}$ final state is indistinguishable from the final state of single t quark production which give rise to interference terms. The contribution from single top events can be reduced by adequate kinematic cuts. Still, future studies will have to consider the residual contribution.

4 Concluding remarks

The t quark could be a window to new physics associated with light composite Higgs bosons and strong coupling in the Higgs sector. The key parameters here are the electro-weak couplings of the t quark. We have demonstrated that the ILC offers unique capabilities to access these couplings and measure them to the required high level of precision. The mass of the t quark, which is a most important quantity in many theories can be measured model independent to a precision of better than 100 MeV. It has however to be pointed out that all of these precision measurements require a superb detector performance and event reconstruction. The key requirements are the tagging of final state b quarks with an efficiency and purity of better than 90% and jet energy reconstruction using particle flow of about 4% in the entire accessible energy range. These requirements are met for the ILC detectors described in the detector volume of [49].

On the other hand the physics program require state-of-the art theoretical calculations for the observables. While QCD corrections seem to be largely under control,

future work should, at least w.r.t the form factors, address the uncertainties on the NLO electroweak corrections. For meaningful experimental studies the existing event generators will have to actively supported.

The full exploitation of the potential of t quark physics at the ILC requires a very close collaboration between theoretical and experimental groups over the coming years. The points outlined in this contribution may serve as a basis for the establishment of such a collaboration.

References

- [1] H. Baer, T. Barklow, K. Fujii, Y. Gao, A. Hoang, *et al.*, “The International Linear Collider Technical Design Report - Volume 2: Physics” [arXiv:1306.6352](#) [[hep-ph](#)].
- [2] **CDF Collaboration**, F. Abe *et al.*, “Observation of top quark production in $\bar{p}p$ collisions” *Phys.Rev.Lett.* **74** (1995) 2626–2631, [arXiv:hep-ex/9503002](#) [[hep-ex](#)].
- [3] **D0 Collaboration**, S. Abachi *et al.*, “Observation of the top quark” *Phys.Rev.Lett.* **74** (1995) 2632–2637, [arXiv:hep-ex/9503003](#) [[hep-ex](#)].
- [4] **CDF Collaboration**, T. Aaltonen *et al.*, “First Measurement of the Ratio $\sigma(t\bar{t})/\sigma(Z/\gamma^{**} \rightarrow \ell\ell)$ and Precise Extraction of the $t\bar{t}$ Cross Section” *Phys.Rev.Lett.* **105** (2010) 012001, [arXiv:1004.3224](#) [[hep-ex](#)].
- [5] **D0 Collaboration**, V. M. Abazov *et al.*, “Measurement of the top quark pair production cross section in the lepton+jets channel in proton-antiproton collisions at $\sqrt{s}=1.96$ TeV” *Phys.Rev.* **D84** (2011) 012008, [arXiv:1101.0124](#) [[hep-ex](#)].
- [6] “Statistical combination of top quark pair production cross-section measurements using dilepton, single-lepton, and all-hadronic final states at $\sqrt{s} = 7$ tev with the atlas detector” Tech. Rep. ATLAS-CONF-2012-024, CERN, Geneva, Mar, 2012.
- [7] “Measurement of the top quark pair production cross section in the single-lepton channel with atlas in proton-proton collisions at 8 tev using kinematic fits with b-tagging” Tech. Rep. ATLAS-CONF-2012-149, CERN, Geneva, Nov, 2012.
- [8] **CMS Collaboration**, S. Chatrchyan *et al.*, “Measurement of the $t\bar{t}$ production cross section in the dilepton channel in pp collisions at $\sqrt{s} = 7$ TeV” *JHEP* **1211** (2012) 067, [arXiv:1208.2671](#) [[hep-ex](#)].
- [9] “Top pair cross section in dileptons” Tech. Rep. CMS-PAS-TOP-12-007, CERN, Geneva, 2012.
- [10] **Tevatron Electroweak Working Group, CDF, D0 Collaborations**, “Combination of CDF and DO results on the mass of the top quark using up to 8.7fb^{-1} at the Tevatron” [arXiv:1305.3929](#) [[hep-ex](#)].
- [11] **ATLAS Collaboration**, “Combination of ATLAS and CMS results on the mass of the top quark using up to 4.9 fb1 of data” *ATLAS-CONF-2012-095*, *ATLAS-COM-CONF-2012-003* (2012) .
- [12] **CDF Collaboration**, “A Direct Top Quark Width Measurement at CDF”. [CDFNote10936](#), http://www-cdf.fnal.gov/physics/new/top/2012/TMT_width_p38/publicnote.pdf.

- [13] **DO Collaboration**, V. M. Abazov *et al.*, “Determination of the width of the top quark” *Phys.Rev.Lett.* **106** (2011) 022001, [arXiv:1009.5686 \[hep-ex\]](#).
- [14] **CDF Collaboration**, “Measurement of $R = B(t \rightarrow Wb)/B(t \rightarrow Wq)$ in the SecVtx tagged lepton plus jets sample with 8.7 fb^{-1} of Data”. [CDFNote10887](#), http://www-cdf.fnal.gov/physics/new/top/confNotes/cdf10887_BRratio8.7fb.pdf.
- [15] **DO Collaboration**, V. Abazov *et al.*, “Precision measurement of the ratio $B(t \rightarrow Wb)/B(t \rightarrow Wq)$ and Extraction of V_{tb} ” *Phys.Rev.Lett.* **107** (2011) 121802, [arXiv:1106.5436 \[hep-ex\]](#).
- [16] “Measurement of the ratio $b(t \rightarrow wb)/b(t \rightarrow wq)$ ” Tech. Rep. CMS-PAS-TOP-12-035, CERN, Geneva, 2013.
- [17] **CDF Collaboration**. [CDF-Note10807](#), http://www-cdf.fnal.gov/physics/new/top/2012/LepJet_AFB_Winter2012/CDF10807.pdf.
- [18] **DO Collaboration**, V. M. Abazov *et al.*, “Forward-backward asymmetry in top quark-antiquark production” *Phys.Rev.* **D84** (2011) 112005, [arXiv:1107.4995 \[hep-ex\]](#).
- [19] **ATLAS Collaboration**, G. Aad *et al.*, “Measurement of the charge asymmetry in top quark pair production in pp collisions at $\sqrt{s} = 7$ TeV using the ATLAS detector” *Eur.Phys.J.* **C72** (2012) 2039, [arXiv:1203.4211 \[hep-ex\]](#).
- [20] **CMS Collaboration**, S. Chatrchyan *et al.*, “Measurement of the charge asymmetry in top-quark pair production in proton-proton collisions at $\sqrt{s} = 7$ TeV” *Phys.Lett.* **B709** (2012) 28–49, [arXiv:1112.5100 \[hep-ex\]](#).
- [21] **CDF Collaboration**, T. Aaltonen *et al.*, “Measurement of W -Boson Polarization in Top-quark Decay using the Full CDF Run II Data Set” *Phys.Rev.* **D87** (2013) 031104, [arXiv:1211.4523 \[hep-ex\]](#).
- [22] **ATLAS Collaboration**, G. Aad *et al.*, “Measurement of the W boson polarization in top quark decays with the ATLAS detector” *JHEP* **1206** (2012) 088, [arXiv:1205.2484 \[hep-ex\]](#).
- [23] “Measurement of w -polarization in di-leptonic $t\bar{t}$ events in pp collisions with $\sqrt{s} = 7$ tev” Tech. Rep. CMS-PAS-TOP-12-015, CERN, Geneva, 2013.
- [24] A. Hoang, M. Beneke, K. Melnikov, T. Nagano, A. Ota, *et al.*, “Top - anti-top pair production close to threshold: Synopsis of recent NNLO results” *Eur.Phys.J.direct* **C2** (2000) 1, [arXiv:hep-ph/0001286 \[hep-ph\]](#).
- [25] M. Beneke and Y. Kiyo, “Ultrasoft contribution to heavy-quark pair production near threshold” *Phys.Lett.* **B668** (2008) 143–147, [arXiv:0804.4004 \[hep-ph\]](#).
- [26] A. Hoang, A. Manohar, I. W. Stewart, and T. Teubner, “The Threshold t anti- t cross-section at NNLL order” *Phys.Rev.* **D65** (2002) 014014, [arXiv:hep-ph/0107144 \[hep-ph\]](#).
- [27] A. H. Hoang, “Three loop anomalous dimension of the heavy quark pair production current in nonrelativistic QCD” *Phys.Rev.* **D69** (2004) 034009, [arXiv:hep-ph/0307376 \[hep-ph\]](#).
- [28] A. Pineda and A. Signer, “Heavy Quark Pair Production near Threshold with Potential Non-Relativistic QCD” *Nucl.Phys.* **B762** (2007) 67–94, [arXiv:hep-ph/0607239 \[hep-ph\]](#).
- [29] A. H. Hoang and M. Stahlhofen, “Two-loop ultrasoft running of the $O(v^2)$ QCD quark potentials” *Phys.Rev.* **D75** (2007) 054025, [arXiv:hep-ph/0611292 \[hep-ph\]](#).

- [30] A. Pineda, “Next-to-leading ultrasoft running of the heavy quarkonium potentials and spectrum: Spin-independent case” *Phys.Rev.* **D84** (2011) 014012, [arXiv:1101.3269 \[hep-ph\]](#).
- [31] A. H. Hoang and M. Stahlhofen, “Ultrasoft NLL Running of the Nonrelativistic $O(v^2)$ QCD Quark Potential” *JHEP* **1106** (2011) 088, [arXiv:1102.0269 \[hep-ph\]](#).
- [32] M. Stahlhofen. Talk given at top physics workshop, paris, may 2012. <http://indico2.lal.in2p3.fr/indico/conferenceOtherViews.py?view=standard&confId=180>.
- [33] M. Beneke, B. Jantzen, and P. Ruiz-Femenia, “Electroweak non-resonant NLO corrections to $e^+e^- \rightarrow W^+W^-b\bar{b}$ in the $t\bar{t}$ resonance region” *Nucl.Phys.* **B840** (2010) 186–213, [arXiv:1004.2188 \[hep-ph\]](#).
- [34] A. A. Penin and J. H. Piclum, “Threshold production of unstable top” *JHEP* **1201** (2012) 034, [arXiv:1110.1970 \[hep-ph\]](#).
- [35] A. H. Hoang, C. J. Reisser, and P. Ruiz-Femenia, “Phase Space Matching and Finite Lifetime Effects for Top-Pair Production Close to Threshold” *Phys.Rev.* **D82** (2010) 014005, [arXiv:1002.3223 \[hep-ph\]](#).
- [36] B. Jantzen and P. Ruiz-Femenía, “NNLO non-resonant corrections to threshold top-pair production from e^+e^- : endpoint-singular terms” [arXiv:1307.4337 \[hep-ph\]](#).
- [37] K. Seidel, F. Simon, M. Tesar, and S. Poss, “Top quark mass measurements at and above threshold at CLIC” [arXiv:1303.3758 \[hep-ex\]](#).
- [38] M. Martinez and R. Miquel, “Multiparameter fits to the t anti- t threshold observables at a future e^+e^- linear collider” *Eur.Phys.J.* **C27** (2003) 49–55, [arXiv:hep-ph/0207315 \[hep-ph\]](#).
- [39] A. Hoang and T. Teubner, “Top quark pair production close to threshold: Top mass, width and momentum distribution” *Phys.Rev.* **D60** (1999) 114027, [arXiv:hep-ph/9904468 \[hep-ph\]](#).
- [40] A. Juste, Y. Kiyo, F. Petriello, T. Teubner, K. Agashe, *et al.*, “Report of the 2005 Snowmass top/QCD working group” [arXiv:hep-ph/0601112 \[hep-ph\]](#).
- [41] G. Moortgat-Pick, T. Abe, G. Alexander, B. Ananthanarayan, A. Babich, *et al.*, “The Role of polarized positrons and electrons in revealing fundamental interactions at the linear collider” *Phys.Rept.* **460** (2008) 131–243, [arXiv:hep-ph/0507011 \[hep-ph\]](#).
- [42] L. Randall and R. Sundrum, “A Large mass hierarchy from a small extra dimension” *Phys.Rev.Lett.* **83** (1999) 3370–3373, [arXiv:hep-ph/9905221 \[hep-ph\]](#).
- [43] **ALEPH Collaboration, DELPHI Collaboration, L3 Collaboration, OPAL Collaboration, SLD Collaboration, LEP Electroweak Working Group, SLD Electroweak Group, SLD Heavy Flavour Group**, S. Schael *et al.*, “Precision electroweak measurements on the Z resonance” *Phys.Rept.* **427** (2006) 257–454, [arXiv:hep-ex/0509008 \[hep-ex\]](#).
- [44] S. J. Parke and Y. Shadmi, “Spin correlations in top quark pair production at e^+e^- colliders” *Phys.Lett.* **B387** (1996) 199–206, [arXiv:hep-ph/9606419 \[hep-ph\]](#).
- [45] M. Amjad, M. Boronat, T. Frisson, I. G. Garcia, R. Pöschl, *et al.*, “A precise determination of top quark electro-weak couplings at the ILC operating at $\sqrt{s} = 500$ GeV” [arXiv:1307.8102 \[hep-ex\]](#).

- [46] P. Doublet, *Hadrons in a highly granular SiW ECAL - Top quark production at the ILC*. PhD thesis, Laboratoire de l'Accélérateur Linéaire and Université Paris Sud - Paris XI, 2011. <http://tel.archives-ouvertes.fr/tel-00657967>.
- [47] E. Devetak, A. Nomerotski, and M. Peskin, “Top quark anomalous couplings at the International Linear Collider” *Phys.Rev.* **D84** (2011) 034029, [arXiv:1005.1756 \[hep-ex\]](#).
- [48] P. Doublet, F. Richard, R. Pöschl, T. Frisson, and J. Rouëné, “Determination of Top-quark Asymmetries at the ILC” [arXiv:1202.6659 \[hep-ex\]](#).
- [49] T. Behnke *et al.*, “ILC TDR and DBD” *ILC-Report-2013-040* (2013) .
- [50] E. L. Berger, Q.-H. Cao, C.-R. Chen, J.-H. Yu, and H. Zhang, “The Top Quark Production Asymmetries A_{FB}^t and A_{FB}^ℓ ” *Phys.Rev.Lett.* **108** (2012) 072002, [arXiv:1201.1790 \[hep-ph\]](#).
- [51] **ECFA/DESY LC Physics Working Group**, J. Aguilar-Saavedra *et al.*, “TESLA: The Superconducting electron positron linear collider with an integrated x-ray laser laboratory. Technical design report. Part 3. Physics at an e+ e- linear collider” [arXiv:hep-ph/0106315 \[hep-ph\]](#).
- [52] **American Linear Collider Working Group Collaboration**, T. Abe *et al.*, “Linear Collider Physics Resource Book for Snowmass 2001 - Part 3” [arXiv:hep-ex/0106057](#).
- [53] U. Baur, A. Juste, L. Orr, and D. Rainwater, “Probing electroweak top quark couplings at hadron colliders” *Phys.Rev.* **D71** (2005) 054013, [arXiv:hep-ph/0412021 \[hep-ph\]](#).
- [54] **CMS Collaboration**, S. Chatrchyan *et al.*, “Measurement of associated production of vector bosons and top quark-antiquark pairs at $\sqrt{s} = 7$ TeV” *Phys.Rev.Lett.* **110** (2013) 172002, [arXiv:1303.3239 \[hep-ex\]](#).
- [55] A. Pomarol and J. Serra, “Top Quark Compositeness: Feasibility and Implications” *Phys.Rev.* **D78** (2008) 074026, [arXiv:0806.3247 \[hep-ph\]](#).
- [56] A. Djouadi, G. Moreau, and F. Richard, “Resolving the A(FB)**b puzzle in an extra dimensional model with an extended gauge structure” *Nucl.Phys.* **B773** (2007) 43–64, [arXiv:hep-ph/0610173 \[hep-ph\]](#).
- [57] Y. Hosotani and M. Mabe, “Higgs boson mass and electroweak-gravity hierarchy from dynamical gauge-Higgs unification in the warped spacetime” *Phys.Lett.* **B615** (2005) 257–265, [arXiv:hep-ph/0503020 \[hep-ph\]](#).
- [58] Y. Cui, T. Gherghetta, and J. Stokes, “Fermion Masses in Emergent Electroweak Symmetry Breaking” *JHEP* **1012** (2010) 075, [arXiv:1006.3322 \[hep-ph\]](#).
- [59] M. S. Carena, E. Ponton, J. Santiago, and C. E. Wagner, “Light Kaluza Klein States in Randall-Sundrum Models with Custodial SU(2)” *Nucl.Phys.* **B759** (2006) 202–227, [arXiv:hep-ph/0607106 \[hep-ph\]](#).
- [60] C. Grojean, O. Matsedonskyi, and G. Panico, “Light top partners and precision physics” [arXiv:1306.4655 \[hep-ph\]](#).
- [61] C. Berger, M. Perelstein, and F. Petriello, “Top quark properties in little Higgs models” [arXiv:hep-ph/0512053 \[hep-ph\]](#).
- [62] J. Fleischer, A. Leike, T. Riemann, and A. Werthenbach, “Electroweak one loop corrections for e+ e- annihilation into t anti-top including hard bremsstrahlung” *Eur.Phys.J.* **C31** (2003) 37–56, [arXiv:hep-ph/0302259 \[hep-ph\]](#).

- [63] P. Khiem, J. Fujimoto, T. Ishikawa, T. Kaneko, K. Kato, *et al.*, “Full $\mathcal{O}(\alpha)$ electroweak radiative corrections to $e^+e^- \rightarrow t\bar{t}\gamma$ with GRACE-Loop” [arXiv:1211.1112](#) [hep-ph].
- [64] W. Kilian, T. Ohl, and J. Reuter, “WHIZARD: Simulating Multi-Particle Processes at LHC and ILC” *Eur.Phys.J.* **C71** (2011) 1742, [arXiv:0708.4233](#) [hep-ph].
- [65] M. Moretti, T. Ohl, and J. Reuter, “O’Mega: An Optimizing matrix element generator” [arXiv:hep-ph/0102195](#) [hep-ph].